

# Time-domain measurement of driven ferromagnetic resonance

Y. Guan and W. E. Bailey

*Materials Science Program, Department of Applied Physics, Columbia University, New York, New York 10027*

E. Vescovo, C.-C. Kao, and D. A. Arena

*National Synchrotron Light Source, Brookhaven National Laboratory, Upton, New York 11973*

(Dated: March 23, 2022)

We present a time-resolved measurement of magnetization dynamics during ferromagnetic resonance (FMR) in a single layer of  $\text{Ni}_{81}\text{Fe}_{19}$ . Small-angle ( $<1^\circ$ ) precession of elemental Ni, Fe moments could be measured directly and quantitatively using time-resolved x-ray magnetic circular dichroism (XMCD) in transmission. The high temporal and rotational sensitivity of this technique has allowed characterization of the phase and amplitude of driven FMR motion at 2.3 GHz, verifying basic expectations for a driven resonance.

Ferromagnetic resonance (FMR) is a venerable topic in the study of magnetism. In the modern technological context, resonance and relaxation underpin the switching response of spin electronic devices at 1 GHz and above.

In this Letter, we demonstrate a time- and element-resolved measurement of ferromagnetic resonance in a single layer of  $\text{Ni}_{81}\text{Fe}_{19}$ . Conventional, low-angle ( $\sim 0.1$ - $1.0^\circ$ ) FMR motion, driven with a continuous wave (CW) low-power microwave field at 2.3 GHz, has been measured in the time-domain using time-resolved x-ray magnetic circular dichroism (XMCD).

Two innovations have allowed the rotational and spatial resolution necessary for the measurement. High magnetic contrast is provided by transmission geometry XMCD(1; 2), the soft x-ray equivalent of Faraday rotation. Cone angles could be measured down to  $0.1^\circ$ . Improved temporal resolution is provided using phase-locked CW microwaves as an excitation source, suppressing the effects of timing jitter present in pulsed experiments(3; 4). Motional and phase resolutions are an order of magnitude better than we achieved in previous work(4) using pulsed step fields in XMCD reflectivity.

In general, magnetization dynamics are described by the Landau-Lifshitz (LL) equation(5), given in SI as

$$\frac{d\mathbf{M}}{dt} = -\mu_0 |\gamma| (\mathbf{M} \times \mathbf{H}) - \frac{\lambda}{M_s^2} (\mathbf{M} \times \mathbf{M} \times \mathbf{H}), \quad (1)$$

where  $\lambda$  is the LL relaxation rate in  $\text{sec}^{-1}$ .

The LL equation can be linearized for small rotations of  $\vec{M}$  about  $\vec{H}$  as

$$\frac{\partial^2 \phi(t)}{\partial t^2} + \lambda \frac{\partial \phi(t)}{\partial t} + \omega_0^2 \phi(t) = 0, \quad (2)$$

where  $\omega_0^2 = \mu_0^2 \gamma^2 H_{eff} (H_{eff} + M_s)$  (6).

Free oscillations, describing the motion of this damped harmonic oscillator about an equilibrium position, are the starting point for most magneto-optical studies of spin dynamics(3; 4; 7; 8; 9). Rotational displacements about an equilibrium are described by  $\phi$ ;  $\omega_0$  is the circular frequency of ferromagnetic resonance (FMR) and  $2/\lambda$  is its characteristic relaxation time.

If instead the motion is forced by a transverse ac field  $H_y(t) = H_{y0} \exp(i\omega t)$ , the response is given as

$$\frac{\partial^2 \phi(t)}{\partial t^2} + \lambda \frac{\partial \phi(t)}{\partial t} + \omega_0^2 \phi(t) = A \exp(i\omega t), \quad (3)$$

where  $A \approx \mu_0^2 \gamma^2 M_s H_{y0}$ . Solving Eq. (3) using  $\phi(t) = \phi_0 \exp(i\omega t) = |\phi_0| \exp[i(\omega t + \delta)]$ , then

$$\phi_0 = \frac{A}{(\omega_0^2 - \omega^2)^2 + \lambda^2 \omega^2} [(\omega_0^2 - \omega^2) - i\omega\lambda]. \quad (4)$$

Thus, the phase  $\delta$  and the amplitude of driven FMR precession can be expressed as:

$$\tan \delta = \frac{-\lambda\omega}{\omega_0^2 - \omega^2}, \quad (5)$$

$$|\phi_0| = \frac{A}{\sqrt{(\omega_0^2 - \omega^2)^2 + \lambda^2 \omega^2}}. \quad (6)$$

These relationships can now be tested directly. Moreover, using *in-situ* FMR (microwave absorption) measurement, the damping  $\lambda$  can be estimated directly through the field linewidth, allowing for a parameter-free comparison with Eqs. (5) and (6).

FMR absorption is given by the imaginary part of the susceptibility,  $\chi''$ , along the rf driving field,  $H_y$ , according to Eq. (4). The field-swept resonance linewidth has half-power points at  $\mu_0 \Delta H_{1/2} = 2\alpha\omega/\gamma$ , directly proportional to the dimensionless damping constant  $\alpha$ . Between these half-power points, the phase lag  $\delta$  of  $\phi(t)$  with respect to the drive field goes through a change of  $90^\circ$  according to Eq. (5).

In lock-in (derivative) detection of microwave absorption, the inflection points of the Lorentzian line shape are more easily seen. These have a width  $\mu_0 \Delta H_{pp} = (2/\sqrt{3})\alpha\omega/\gamma$ (10). While  $\alpha = \lambda/(\mu_0 M_s \gamma)$  for low damping ( $\alpha \ll 1$ ),  $\lambda$  can thus be expressed as

$$\lambda = \frac{\sqrt{3}}{2} \frac{\mu_0^2 \gamma^2 M_s \Delta H_{pp}}{\omega}. \quad (7)$$

Then, the following relationship can be derived as

$$\sqrt{3}\Delta H_{pp} = \Delta H_{1/2} = \frac{1}{\sqrt{3}}\Delta H_{\frac{1}{2}|\phi_0|}, \quad (8)$$

where  $\Delta H_{\frac{1}{2}|\phi_0|}$  denotes the linewidth defined by the half-amplitude points.

Time-resolved XMCD (TR-XMCD) measurements of magnetization motion during FMR precession were carried out at Beamline 4-ID-C of Advanced Photon Source in Argonne, IL. The circular dichroism signal was obtained in transmission, using photon helicity  $\vec{\sigma}$  switching ( $\vec{\sigma}$ , with an incident angle of  $38^\circ$  from normal, and with in-plane projection along  $\hat{y}$ ) at the elliptical undulator for fixed static applied field  $H_B$ . The transmitted intensity was read at a soft x-ray sensitive photodiode and normalized to an incident intensity at a reference grid.

Transmission measurements require an x-ray transparent sample and substrate. For time-resolved measurements, x-ray transparent RF field delivery system is also necessary. The  $\text{Ni}_{81}\text{Fe}_{19}$ (25nm)/Cu(2nm) thin film sample was deposited onto a Si/Si<sub>3</sub>N<sub>4</sub> membrane using UHV magnetron sputtering at a base pressure of  $4 \times 10^{-9}$  Torr. The sample was placed in the center of a hollow microwave resonator. Uniform precession of the magnetization was excited at 2.3 GHz by a CW low-power microwave field, synchronized with variable delay to APS x-ray photon bunches (88 MHz). Microwave absorption was measured *in-situ*, using standard lock-in techniques, detecting reflected power at the resonator. Orthogonal Helmholtz coils were used to apply longitudinal bias field  $H_B\hat{x}$  or transverse bias field  $H_T\hat{y}$ .

Element-specific XMCD hysteresis loops were taken as a function of transverse bias field  $H_T$  to obtain a calibration for magnetization angle  $\phi$ . Photon energies were set to the  $L_3$  peaks for Fe (707.5 eV) and Ni (852.0 eV) to measure Fe and Ni XMCD signals, respectively. The saturation values of XMCD signals are taken to be  $\phi_{Fe} = \phi_{Ni} = \pm 90^\circ$ .

$L_{2,3}$ -edge XAS and MCD spectra have been measured in transmission for both Fe and Ni in  $\text{Ni}_{81}\text{Fe}_{19}$ . High-quality spectra are obtained here, as shown in our previous work at NSLS, Beamline U4B(2). Fig. 1(a) shows Fe transmission XAS spectra for both photon helicity directions, with the difference. Corresponding spectra for Ni are shown in Fig. 1(b).

Time- and element-resolved XMCD measurements of magnetization precession at resonance are presented in Fig. 2. XMCD signals were taken as a function of delay time and converted into time-dependent elemental magnetization angles  $\phi_{Fe}(t)$  and  $\phi_{Ni}(t)$  for Fe and Ni, respectively(4). Precessional oscillations are clearly seen. Fe and Ni moments are found to precess together within instrumental resolution, improved here to  $\pm 2$  ps and  $< 0.1^\circ$ .

Time-resolved XMCD measurements of magnetization precession off resonance are presented in Fig. 3. Applied fields were selected according to *in-situ* measured FMR spectra (Fig. 4(a)), spanning the resonance condition

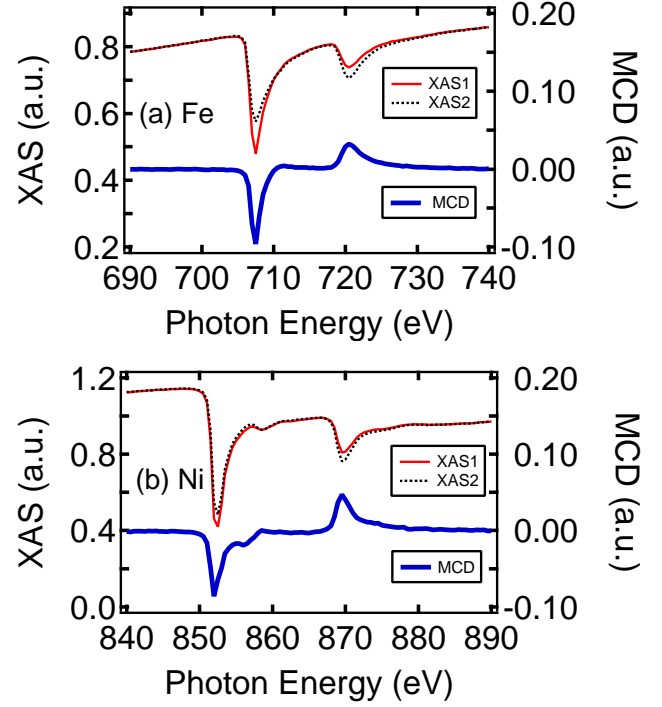


FIG. 1 (a)  $L_{2,3}$ -edge transmission XAS and MCD spectra of Fe in  $\text{Ni}_{81}\text{Fe}_{19}$ ; (b)  $L_{2,3}$ -edge transmission XAS and MCD spectra of Ni in  $\text{Ni}_{81}\text{Fe}_{19}$ .

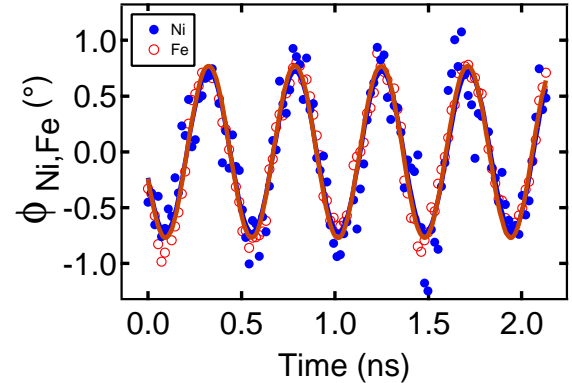


FIG. 2 TR-XMCD measurement of Fe and Ni magnetization precession at resonance, 37 Oe at 2.3 GHz. Solid lines are sinusoidal fits of the Fe and Ni data sets separately.

$H_{res}$  (37 Oe) to  $\sim 4 \times \Delta H_{pp}$  off resonance (5 Oe). A clear variation in the amplitude of driven FMR motion  $\phi_{Fe}(t)$ , and its phase, compared with the RF excitation field, can be seen.

The key result of this letter is presented in Fig. 4(b). Verifying basic expectations of a driven resonance, we can clearly see a  $90^\circ$  phase shift generated through the adjustment of  $\omega_0$  (through longitudinal bias field  $H_B$ ) to  $\ll \omega$ , and a Lorentzian variation of the precessional amplitude. Both behaviors are in excellent agreement with

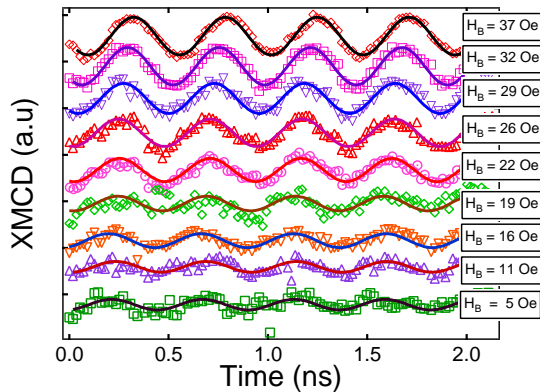


FIG. 3 TR-XMCD measurement of  $\text{Ni}_{81}\text{Fe}_{19}$  magnetization precession off resonance at Fe  $L_3$  edge. Solid lines are sinusoidal fits.

the linearized model (Eqs. (5) and (6)). No empirical parameters have been used apart from  $H_{y0}$ ;  $\lambda$  is estimated as 1.80 GHz directly from the *in-situ* measured FMR spectra (Fig. 4(a)) using Eq. (7). We verify directly the relationship in Eq. (8), with  $\sqrt{3}$  separating the peak-to-peak, 1/2 power ( $90^\circ$  phase shift), and 1/2 amplitude linewidths.

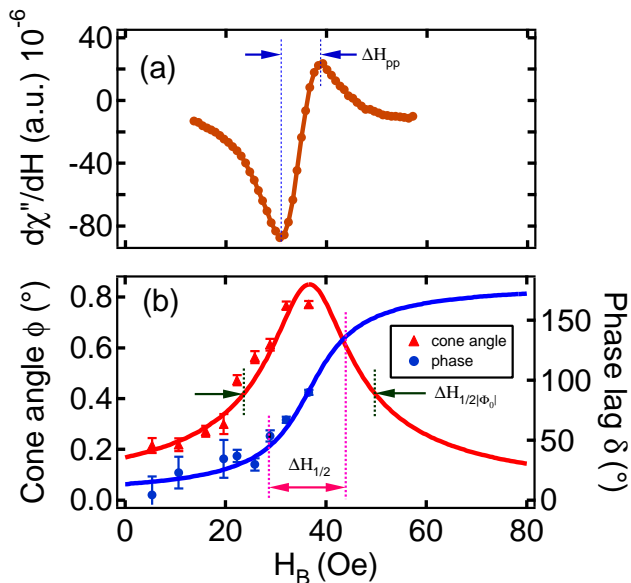


FIG. 4 (a) *In-situ* measurement of FMR spectra of  $\text{Ni}_{81}\text{Fe}_{19}$  by microwave absorption at 2.3 GHz; (b) Measurement of phase and amplitude of driven FMR precession in  $\text{Ni}_{81}\text{Fe}_{19}$  by TR-XMCD. Solid lines are the corresponding theoretical simulations from Eqs. (5) and (6).

In conclusion, we have measured driven ferromagnetic resonance (FMR) precession in the time domain using time-resolved XMCD. Precessional phase and amplitude, lumped together in microwave absorption measurement, could be measured directly, providing a vivid illustration of damped oscillator behavior.

The authors thank Carl Patton for a critical reading of this manuscript, and David J. Keavney (APS) for beamline support. This work was partially supported by the Army Research Office with Grant No. ARO-43986-MS-YIP, and the National Science Foundation with Grant No. NSF-DMR-02-39724. Use of the Advanced Photon Source was supported by the U.S. Department of Energy, Office of Science, Office of Basic Energy Sciences, under Contract No. W-31-109-Eng-38.

## References

- [1] C. Chen, Y. Idzerda, H.-J. Lin, N. Smith, G. Meigs, E. Chaban, G. Ho, E. Pellegrin, and F. Sette, *Phys. Rev. Lett.* **75**, 152 (1995).
- [2] Y. Guan, Z. Dios, D. A. Arena, L. Cheng, and W. E. Bailey, *J. Appl. Phys.* **97**, 10A719 (2005).
- [3] T. Silva, C. Lee, T. Crawford, and C. Rogers, *J. Appl. Phys.* **85**, 7849 (1999).
- [4] W. E. Bailey, L. Cheng, D. J. Keavney, C. -C. kao, E. Vescovo, and D. A. Arena, *Phys. Rev. B* **70**, 172403 (2004).
- [5] L. D. Landau, E. M. Lifshitz, and L. P. Pitaevski, *Statistical Physics, Part 2* (Pergamon, Oxford, 1980).
- [6] Charles Kittel, *Introduction to Solid State Physics* (Wiley, 2005)
- [7] D. M. Engebretson, J. Berezovsky, J. P. Park, L. C. Chen, C. J. Palmstrom, and P. A. Crowell, *J. Appl. Phys.* **91**, 8040 (2002).
- [8] R. Meckenstock, M. Möller, and D. Spoddig, *Appl. Phys. Lett.* **86**, 112506 (2005).
- [9] S. Tamaru, J. A. Bain, R. J. M. van de Veerdonk, T. M. Crawford, M. Covington, and M. H. Kryder, *Phys. Rev. B* **70**, 104416 (2004).
- [10] B. Heinrich, *Ultrathin Magnetic Structures II*, edited by B. Heinrich and J. A. C. Bland (Springer-Verlag, Berlin, 1994).